EASR

Engineering and Applied Science Research

https://www.tci-thaijo.org/index.php/easr/index

Published by the Faculty of Engineering, Khon Kaen University, Thailand

Calculation of optimum interstage pressure of two-stage CO_2 compression using cubic equations of state

Sompop Jarungthammachote*

Department of Mechanical Engineering, Faculty of Engineering at Sriracha, Kasetsart University, Chonburi 20230, Thailand

Received 24 April 2023
Revised 19 October 2023
Accepted 27 October 2023

Abstract

CO_2 has been widely used as a working fluid in power generation and refrigeration systems and multistage compression is one important process in these systems. To save energy consumption, the compression should be conducted at optimum interstage pressure. In this work, a model to find the optimum interstage pressure for two-stage CO_2 compression is studied. Use of cubic equations of state in the model is investigated and compared its result with the result from using a multiparameter equation of state, called SW equation of state. The compression in a subcritical region and from a subcritical to a supercritical region are investigated. The results of this study show that the cubic equations of state, except van der Waals equation of state, can generally predict the CO_2 density and thermal expansivity with satisfied accuracy. The optimum interstage pressures obtained from the model using Redlich-Kwong, Peng-Robinson, and Redlich-Kwong-Soave equations of state are close to that using SW equation of state. The average absolute percentage difference (AAPD) from the comparison showed that these three cubic equations of state have AAPD less than 0.6% and 0.9% for the subcritical and transcritical compressions, respectively. The result of the study also shows that when the optimum interstage pressure is higher than the critical pressure, the optimum interstage pressure slightly increases with increasing the outlet pressure of the second-stage compressor.

Keywords: Cubic equation of state, Optimum interstage pressure, CO_2 compression, Thermal expansivity

1. Introduction

Carbon dioxide (CO_2) is now an interesting gas involving environmental problems, power generation systems, refrigeration systems, chemical industries, etc. CO_2 is a greenhouse gas regarding a main contributor of global warming and climate change. Use of fossil fuels, such as in power generation and transportation sectors, has been the single largest source of CO_2 emissions, responsible for nearly 65% of the global greenhouse gas emissions [1]. The capture and storage of CO_2 from flue gases is considered as one potential way to reduce global CO_2 emissions.

Due to climate change, refrigerants with low ozone depletion potential (ODP) and global warming potential (GWP) are developed. Even the GWP of CO_2 equals one, CO_2 has been interested to use as a refrigerant because of nontoxic, non-flammables, and noncorrosive. Moreover, CO_2 can be obtained as a waste product from some industrial activities, which is good for the environment [2]. As an interesting refrigerant, much effort has been paid to improving the CO_2 refrigeration cycle's performance in recent years [3].

In power generation, the supercritical CO_2 Brayton cycle technology has been widely studied as it has high efficiency, low corrosion rate and compact system layout [4]. Another advantage of using supercritical CO_2 in the Brayton cycle is that the higher density at the compressor inlet reduces the compressor specific work [5]. A review of supercritical CO_2 power cycle integrated with concentrating solar power and the discussion of supercritical CO_2 properties can be found in [6].

Compression is an important process in the operation of such systems mentioned above. To compress CO_2 gas from a low pressure to a desired pressure, a multistage compression has been often used. Intercooling processes have been applied between compression stages. An optimum interstage pressure, so called an intermediate pressure, is a critical parameter of a two-stage compression system [7] because it leads to a minimum specific compression work. Textbooks [8, 9] usually used an ideal gas with constant specific heat to find the optimum interstage pressure and the suction temperature of the second-stage compressor is cooled down to that of the first-stage compressor. The optimum interstage pressure based on the ideal gas model is:

$$P_{opt,id} = \sqrt{P_i P_o} \tag{1}$$

where P_i represents the suction pressure of the first-stage compressor and P_o is the discharge pressure of the second-stage compressor. Equation (1) expresses that the optimum interstage pressure is the geometric mean of the suction and discharge pressures and this

*Corresponding author.
Email address: Sompop.j@ku.th
doi: 10.14456/easr.2024.1

optimum interstage pressure causes the same compression ratio in the first stage and the second-stage compressions. However, Özgür [10] has discussed that the ideal gas model may not provide the optimum interstage pressure in practice. The optimum interstage pressure from the ideal gas model can be used as a good initial guess for an iterative method to find the optimum interstage pressure [11].

A better ideal gas model to determine the optimum interstage pressures in the multistage compression has been developed by Vadasz and Weiner [12]. The difference of suction gas temperatures and the pressure drops in intercoolers were considered in their model. A similar result of the optimum interstage pressures, expressed in Vadasz and Weine's work, has been found in a study from Lugo-Méndez et al. [13]. Different calculation methods of the optimum interstage pressure, however, based on the ideal gas assumption, have been found in literature [14, 15].

The optimum interstage pressure has been usually obtained using the mathematical concept of finding a maximum or minimum point. To find the optimum thermodynamic condition in refrigeration systems, the derivative of the COP (coefficient of performance) with respect to a pressure is found and it is set to be zero to find the pressure giving the maximum COP [16-18]. Inversely, the minimum compression specific work can be found by setting the derivative of the specific work with respect to the pressure [19]. In these methods, the thermodynamic properties of real gases, such as enthalpy and density, can be adopted in the calculation and use of real gas properties in the calculation is better than using ideal gas assumption. However, the differentiations of thermodynamic properties must appear in the calculations and these terms cause complicated calculations [16]. Computer simulation programs and commercial computer programs providing thermodynamic properties are sometimes required such as those programs applied in the works from [17, 18].

Thermodynamic properties of CO_2 can be calculated using an equation of states. A multiparameter equation of state called Span and Wagner (SW) equation of state [20] is an accurate equation of state and known as an international reference equation of state for CO_2 covering a wide range of temperature and pressure [21]. However, due to complication and time consumption, SW equation of state is not included in most of the commercial software package [22]. Jarungthammachote [23] has developed a calculation model of the optimum interstage pressures for multistage compression with intercoolings. The focused compression range of the study was mainly in the supercritical region. The model expressed in terms of real gas properties and a partial derivative of entropy. Multiparameter equations of state for different gases were used to find the properties and the derivative term in the study. The author has mentioned that the multiparameter equations of state can give accurate properties of the gases even in supercritical region. However, they consume computational resources and time. This is because a multiparameter equation of state consists of many terms and some are complicated exponential terms. From this disadvantage, use of other equations of state should be studies and cubic equations of state are interesting choices for this purpose. Calculation of properties using cubic equations of state shows some advantages over using other types of equation of state. Cubic equations of state are relatively simple as they involve only a few parameters. Moreover, these parameters can be easily adjusted and fitted to experimental data allowing for improved accuracy when modeling the properties of specific gases or mixtures. The cubic equations of state are simple and easier for coding to develop a mathematical model and this simplicity leads to an efficient computation of properties. The cubic equations of state, such as Peng-Robinson (PR) and Redlich-Kong-Soave (RKS) equations of state, have been employed to find CO_2 and other gases properties in single-phase regions, i.e., superheated and supercritical regions [24-29]. Based on the literature [24, 27-29], PR and RKS equations of state can give sufficient accurate results in prediction of density and other properties of CO_2 in superheated and supercritical regions. Therefore, the cubic equations of state should be investigated about their applications in the development of the optimum interstage pressure model.

This study aims to develop a model for calculation of the optimum interstage pressure in two-stage CO_2 compression with an intercooling process. The model is based on use of cubic equations of state, there are van der Waals (vdW), Redlich-Kwong (RK), PR, and RKS equations of state. The properties of CO_2 used to find the optimum interstage pressure obtained from the cubic equations of state are validated with SW equation of state as well as experimental data. The model is investigated for CO_2 compression in superheated region (subcritical compression) and superheated to supercritical region (transcritical compression). The results of the model are compared with that from the previous model which used SW equation of state. This work contributes the alternative way to find the optimum interstage pressure of two-stage CO_2 compression, which is based on the real gas properties. It is, therefore, better than use of ideal gas model, especially in the transcritical compression. Moreover, it can indicate the potential of cubic equations of state application for the optimum interstage pressure model.

2. Materials and methods

2.1 Equation of state

In this study, four cubic equations of state, vdW, RK, PR, and RK equations of state, are focused. The reference equation of state used in this study is SW equation of state. A general format of the cubic equations of state can be presented as

$$P = \frac{RT}{v-b} - \frac{a}{(v+c)(v+d)} \tag{2}$$

The parameters a, b, c and d are described in Table 1. P_c, T_c and ω are the critical pressure, the critical temperature, and the acentric fraction, respectively. The values of P_c, T_c and ω used in this study are P_c =7.3773 MPa, T_c =304.1282 K and ω = 0.22394. R is the gas constant and its value for CO_2 is R = 0.18892 kJ/kg·K.

Table 1 Parameters for the cubic equations of state

Equation of state	*a*	*b*	*c*	*d*
vdW	$\frac{27}{64}\frac{R^2T_c^2}{P_c}$	$\frac{1}{8}\frac{RT_C}{P_C}$	0	0
RK	$0.42748\frac{R^2T_c^2}{P_c}\frac{1}{\sqrt{T_r}}$	$0.08664\frac{RT_C}{P_C}$	b	0
PR	$0.45724\frac{R^2T_c^2}{P_c}\alpha$ $\alpha=\left[1+m\left(1-\sqrt{T_r}\right)\right]^2,$ $m=0.37464+1.54226\omega-0.26992\omega^2$	$0.07780\frac{RT_C}{P_C}$	$\left(1+\sqrt{2}\right)b$	$\left(1-\sqrt{2}\right)b$
RKS	$0.42748\frac{R^2T_c^2}{P_c}\alpha$ $\alpha=\left[1+m\left(1-\sqrt{T_r}\right)\right]^2,$ $m=0.48508+1.5517\omega-0.15613\omega^2$	$0.08664\frac{RT_C}{P_C}$	b	0

To find the specific volume, which is an inverse of density, a cubic equation of specific volume, is obtained as.

$$v^3+\left(c+d-b-\frac{RT}{P}\right)v^2+\left[\frac{a}{P}-\left(\frac{RT}{P}+b\right)(c+d)+cd\right]v-\left[\frac{ab}{P}+\left(\frac{RT}{P}+b\right)(cd)\right]=0 \tag{3}$$

The SW equation of state is the multiparameter equation of state which is possibly classified as a Helmholtz-type equation of state. The specific Helmholtz free energy, $a(\rho,T)$, is presented in terms of a non-dimensional Helmholtz free energy, $\phi(\delta,\tau)$, and it is split into an ideal gas part, $\phi^o(\delta,\tau)$, and a residual part, $\phi^r(\delta,\tau)$, as shown in Eq. (4).

$$\phi(\delta,\tau)=\frac{a(\rho,T)}{RT}=\phi^O(\delta,\tau)+\phi^r(\delta,\tau) \tag{4}$$

where $\delta=\rho/\rho_c$ and $\tau=T_c/T$ are the reduced density and the inverse of reduced temperature, respectively. The subscript c denotes the value at the critical point. The details of SW equation of state can be found in [20].

2.2 Optimum interstage pressure of CO_2 compression

For a two-stage compression with an intercooling process, the total specific work can be determined as:

$$w_{tot}=\frac{(h_{4,s}-h_3)}{\eta_{isen2}}+\frac{(h_{2,s}-h_1)}{\eta_{isen1}} \tag{5}$$

where the subscript s represents the isentropic process and the subscripts 1, 2, 3 and 4 indicate the thermodynamic states in the two-stage compression shown in Figure 1.

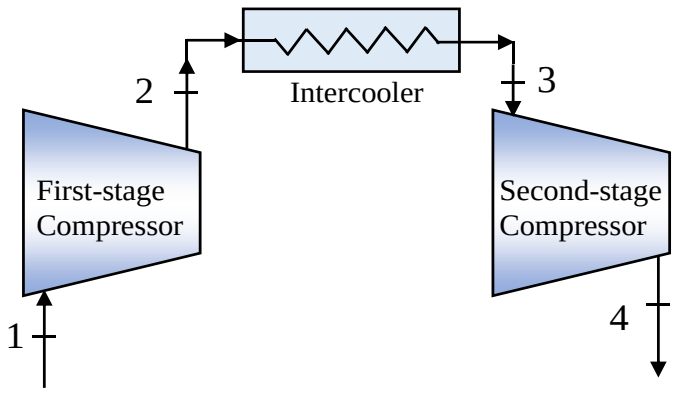

Figure 1 Two-stage compression with intercooling process

In this study, no pressure losses in the intercooler and pipelines and the constant isentropic efficiencies of η_{isen1} and η_{isen2}, are assumed in the analysis. To find the optimum interstage pressure, $P_{2opt} = P_{3opt}$, the derivative of the total specific work with respect to P_2 is determined and set to be zero. It finally results:

$$\frac{T_4 - T_3}{\eta_{isen2}} - \frac{\left[1/(\rho_3\eta_{isen2}) - 1/(\rho_2\eta_{isen1})\right]}{\left(\partial s_3/\partial P_3\right)_{T=T_3}} = 0 \tag{6}$$

A detail of derivation of Eq. (6) is shown in Appendix A. Based on the Maxwell relation, the denominator of the second term, $(\partial s/\partial P)_T$, can be replaced by $-(\partial v/\partial T)_P$ and this derivative can relate to a fluid property called the thermal expansivity (or the thermal expansion coefficient), β, which is defined as:

$$\beta = \frac{1}{v}\left(\frac{\partial v}{\partial T}\right)_P = -\frac{1}{\rho}\left(\frac{\partial \rho}{\partial T}\right)_P = \frac{1}{v}\left[\frac{\left(\partial P/\partial T\right)_v}{\left(\partial P/\partial v\right)_T}\right] \tag{7}$$

Thus, Eq. (6) can be rewritten as:

$$f = T_4 - T_3 + \left[1 - \frac{\rho_3}{\rho_2}\frac{\eta_{isen2}}{\eta_{isen1}}\right]\frac{1}{\beta_3} = 0 \tag{8}$$

2.3 Thermodynamic properties

To find the optimum interstage pressure using Eq. (8) the density and thermal expansivity of CO_2 are required. The density is an inverse of the specific volume, obtained from solving Eq. (3). The thermal expansivity can be calculated from the most-right term in Eq. (7) because the cubic equations of state are explicitly expressed in terms of pressure. The derivative terms, $(\partial P/\partial T)_v$ and $(\partial P/\partial v)_T$, obtained from the cubic equations of state as well as SW equation of state, are shown in Table 2. In the case of SW equation of state, the details of partial derivative terms can be found in Span and Wagner's work [20].

Table 2 The derivative terms in Eq. (7) calculated using cubic and SW equations of state

Equation of state	$(\partial P/\partial T)_v$	$(\partial P/\partial v)_T$
vdW	$\frac{R}{(v-b)}$	$\frac{-R}{(v-b)^2} + \frac{2a}{v^3}$
RK	$\frac{R}{(v-b)} + \frac{a}{2v(v+b)T}$	$\frac{-R}{(v-b)^2} + \frac{a(2v+b)}{v^2(v+b)^2}$
PR	$\frac{R}{(v-b)} + \frac{am}{\left[v(v+b)+b(v-b)\right]\sqrt{TT_c\alpha}}$	$\frac{-R}{(v-b)^2} + \frac{2a(v+b)}{\left[v(v+b)+b(v-b)\right]^2}$
RKS	$\frac{R}{(v-b)} + \frac{am}{v(v+b)\sqrt{TT_c\alpha}}$	$\frac{-R}{(v-b)^2} + \frac{a(2v+b)}{v^2(v+b)^2}$
SW	$\rho R\left(1 + \delta\frac{\partial \phi^r}{\partial \delta} - \tau\delta\frac{\partial^2 \phi^r}{\partial \delta \partial \tau}\right)$	$TR\left(1 + 2\delta\frac{\partial \phi^r}{\partial \delta} + \delta^2\frac{\partial^2 \phi^r}{\partial \delta^2}\right)$

The value of entropy used in the isentropic process calculation is obtained from the dimensionless entropy departure, $(s - s^{ig})/R$, and it can be computed based on the cubic equations of state as presented in Table 3. The standard entropy available in NASA report [30] is used to find the ideal gas entropy, s^{ig}.

Table 3 Dimensionless entropy departure obtained from the cubic equations of state

Equation of state	$(s - s^{ig})/R$
vdW	$\ln\left[Z(1-b/v)\right]$
RK	$\ln\left[Z(1-b/v)\right] - \frac{a}{2bRT}\ln(1+b/v)$
PR	$\ln\left[Z(1-b/v)\right] - \frac{da/dT}{2\sqrt{2}\,bR}\ln\left[\frac{1+\left(1+\sqrt{2}\right)b/v}{1+\left(1-\sqrt{2}\right)b/v}\right]$, $da/dT = -\frac{am}{\sqrt{TT_c\alpha}}$
RKS	$\ln\left[Z(1-b/v)\right] - \frac{da/dT}{bR}\ln(1+b/v)$, $da/dT = -\frac{am}{\sqrt{TT_c\alpha}}$

2.4 Calculation of the optimum interstage pressure

The calculation procedure to find the optimum interstage pressure using the cubic equations of state is shown in Figure 2. Hereafter, the symbol EoS represents the word "equation of state". The ideal gas optimum interstage pressure multiplied with a constant c, $P_{2,init} = c\sqrt{P_{in}P_{out}}$, can be used as the initial guess of P_2. The constant can be varied between 1.3 to 1.6. The recommended value of c was obtained from the fact that the ideal gas model usually underestimates the optimum interstage pressure and based on the pressure and temperature ranges in this study, the ratio of optimum interstage pressure from the ideal gas model and that from the cubic equations of state generally varied from 1.3 to 1.6.

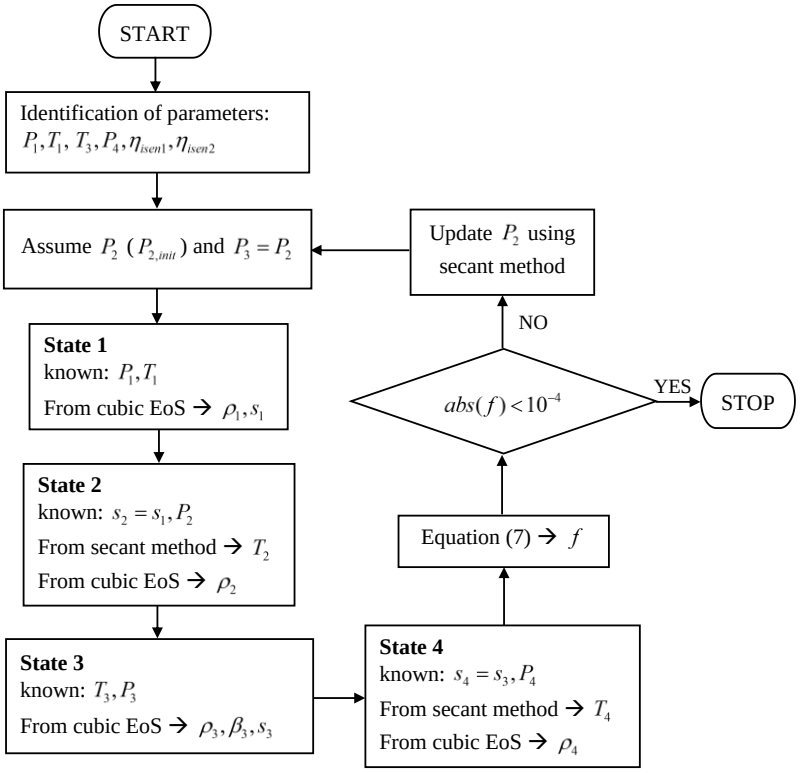

Figure 2 Calculation procedure of optimum interstage pressure

3. Results and discussion

3.1 Density and thermal expansivity comparisons

In this section, the density and the thermal expansivity calculated from the cubic equations of state are compared to that calculated from SW equation of state. For the density, the calculation results from the cubic equations of state are also compared to the experimental data. The comparisons are done in 3 regions. The first (I) and second (II) regions are superheated with $T < T_c$ and $T_c < T$, respectively. The third (III) region is a supercritical region. The details of each comparison region are shown in Table 4. The average absolute percentage deviation ($AAPD$) is used in the comparisons. The formula of $AAPD$ is expressed in Eq. (9) and it is the average value of the absolute percentage deviations (APD). In comparison of the density from cubic equations of state with that from the experimental data, ρ^{SW} in Eq. (9) is replaced by the density from the experiment, $\rho^{\exp}$.

$$AAPD = \frac{1}{N}\sum_{i=1}^{N}\frac{\left|\rho_i^{SW} - \rho_i^{cubic}\right|}{\rho_i^{SW}}100 = \frac{1}{N}\sum_{i=1}^{N}APD \tag{9}$$

Table 4 Pressure and temperature ranges and the number of comparison points in each region

Region	Temperature range (K)	Pressure range (MPa)	No. of data points
(I)	222.0 – 302.0	0.599 – 6.713	231
(II)	304.0 – 1000.0	0.599 – 7.370	441
(III)	304.1282 – 1000.0	7.3773 – 60.000	900

Table 5 shows the $AAPD$ obtained from the comparison of density calculated from cubic equations of state and SW equation of state in different regions. In region (I), RKS and PR equations of state give lowest $AAPD$ in density and thermal expansivity comparisons, respectively. For the high temperature superheated region, region (II), PR equation of state can predict the density of CO_2 better than the others, while RKS estimates the thermal expansivity slightly better than PR. However, RK, PR and RKS can predict density and thermal expansivity with slightly different $AAPD$. For vdW equation of state, it provides the density of CO_2 in the superheated regions with highest $AAPD$. If the ideal gas law is applied, it gives the density in the higher temperature superheated region

with $AAPD$ of 3.19%, while $AAPD$ of vdW equation of state is 1.412%. Therefore, use of vdW equation of state to predict the density of CO_2, even in the high temperature region, gives a better result than use of the ideal gas law. The highest $AAPD$ of each cubic equation of state is found in the supercritical region. PR equation of state has considerably low $AAPD$ for density prediction and it also gives the thermal expansivity with the lowest $AAPD$ when compared to other cubic equations of state.

Table 5 $AAPD$of density and thermal expansivity comparisons between that from cubic equations of state and SW equation of state.

EoS	Property	$AAPD$ (%)		
		Region (I)	**Region (II)**	**Region (III)**
vdW	ρ	3.443	1.412	7.744
	β	17.892	2.582	15.228
RK	ρ	1.115	0.799	3.795
	β	8.868	1.011	4.391
PR	ρ	0.751	**0.375**	**0.946**
	β	**2.992**	0.946	**3.177**
RKS	ρ	**0.548**	0.721	4.562
	β	4.077	**0.801**	4.962

To compare the density prediction from the cubic equations of state with that from the experiments, CO_2 densities in superheated and supercritical regions available in the literature [31-33] are used. The experimental data were not recorded in equal increments of temperature and pressure and the experimental data used in the comparison are not cover the pressure and temperature ranges shown in Table 4. In superheated region, the data cover the temperature and pressure ranges of 220 K to 697.81 K and 0.2973 MPa to 7.37163 MPa, respectively. For supercritical region, the densities are available in the temperature and pressure ranges of 304.135 K to 695.36 K and 7.37861 MPa to 34.203 MPa, respectively. The number of experimental data points used in this comparison is totally 485. There are 226 data points located in the superheated region and 259 data points are in the supercritical region. Table 6 expresses $AAPD$ of the comparison between the density predicted from cubic equations of state and that from experiments. The comparison results in Table 6 indicate that PR equation of state gives the lowest $AAPD$ in the comparison of density in superheated and supercritical regions.

Table 6 $AAPD$of the density comparison between that from cubic equations of state and experimental values

EoS	$AAPD$ (%)	
	Superheated region	**Supercritical region**
vdW	5.442	12.287
RK	2.173	6.174
PR	1.280	3.852
RKS	1.693	8.590

3.2 Optimum interstage pressure

To show the optimum interstage pressure calculated from the cubic equations of state, the compressions of CO_2 are classified into two cases, the subcritical and the transcritical compressions. The inlet state, defined by P_1 and T_1, and T_3 of the subcritical compression case are P_1 = 101.325 kPa, T_1 = 298K and T_3 = 306 K, while these of the transcritical compression case are P_1 = 2.6487 MPa, T_1 = 264 K and T_3 = 306 K. The outlet temperature of the intercooler defined at 306 K is based on the concept that the ambient air is used as a cooling fluid. The cooling air has an average temperature of 301 K (28 ^{o}C) and the approach temperature is set at 5 K. The desired pressure, P_4, of these two compression cases is varied to study the change of the optimum interstage pressure. The simulation results are shown in the following sections.

3.2.1 Subcritical compression

For CO_2 subcritical compression, the optimum interstage pressures calculated using the cubic equations of state for the isentropic compression are presented in Figure 3(a). It shows that at low P_4, all cubic equations of state give almost the same optimum interstage pressure. However, when P_4 increases the difference of the optimum interstage pressures obtained from different cubic equations of state can be observed. Among cubic equations of state, PR and RKS equations of state provide virtually the same optimum interstage pressure. For example, at P_4 = 7.0 MPa, the optimum interstage pressure predicted by PR and RKS equations of state are 0.9933 and 0.9912 MPa, respectively. At P_4 = 7.0 MPa, SW equation of state gives the optimum interstage pressure of 0.9857 MPa. The comparison of the optimum interstage pressures from PR and SW equations of state shows the APD of 0.77%, while that from RKS and SW equation of state gives APD of 0.55%. In the case of using RK and vdW equations of state to find the optimal interstage pressure for P_4 = 7.0 MPa, the APD are 0.84% and 2.22%, respectively. The $AAPD$ from the case of PR, PK, and RKS equations of state are slightly different and the $AAPD$ of these three cases are less than 0.6%. Moreover, the ideal gas model, $P_{opt} = \sqrt{P_1 P_4}$, is also used to find the optimum interstate pressures at different P_4 and they are compared with the results of other equations of state as shown in Figure 3(a). It is clearly illustrated that the ideal gas model provides the optimum interstage pressures much lower than that from other equations of state. The $AAPD$ from the comparison of the ideal gas model and SW equation of state is 11.5%.

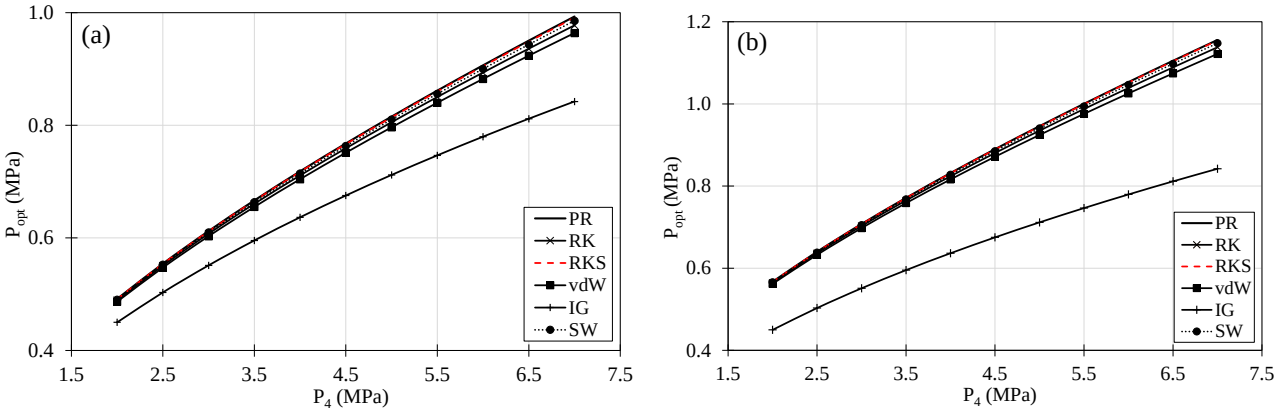

Figure 3 Optimum interstage pressure for CO_2 compression from P_1 = 0.101325 MPa, T_1= 298 K to different P_4 with T_3 = 306 K (a) isentropic compression and (b) non-isentropic compression with $\eta_{isen,1} = 0.87$ and $\eta_{isen,2} = 0.82$

In Figure 3(b), the optimum interstage pressures calculated from the cubic and SW equations of state as well as the ideal gas model for non-isentropic compressions are presented. The isentropic efficiencies are $\eta_{isen,1} = 0.87$ and $\eta_{isen,2} = 0.82$. The results in Figure 3(b) show that the cubic equations of state can give the optimum interstage pressure of non-isentropic compression marginally different from that given by SW equation of state. The $AAPD$ of the comparison for the case of PR, RK, and RKS are 0.49%, 0.54%, and 0.42%, respectively. For vdW equation of state, it has $AAPD$ of the comparison of 1.52%. If the ideal gas model is applied for the non-isentropic compression, it yields $AAPD$ of 23.64%. It should be noted that the ideal gas model is developed based on isentropic compression. Application of ideal gas model in non-isentropic compression can cause a large value of deviation. The total specific compression work computed based on the optimum interstage pressure obtained from PR and RKS equations of state are about the same value as that from SW equation of state and they are a little lower than that from the other cubic equations of state.

3.2.2 Transcritical compression

To study the optimum interstage pressure of CO_2 compression from the subcritical region to the supercritical region, the inlet state is defined as P_1 = 2.6487 MPa, T_1 = 264 K (0.85 degree of superheat) and T_3 is fixed at 306 K. The outlet pressure, P_4, is varied from 7.0 MPa to 15.0 MPa. The optimum interstage pressure of isentropic and non-isentropic compressions are shown in Figures 4(a) and 4(b), respectively.

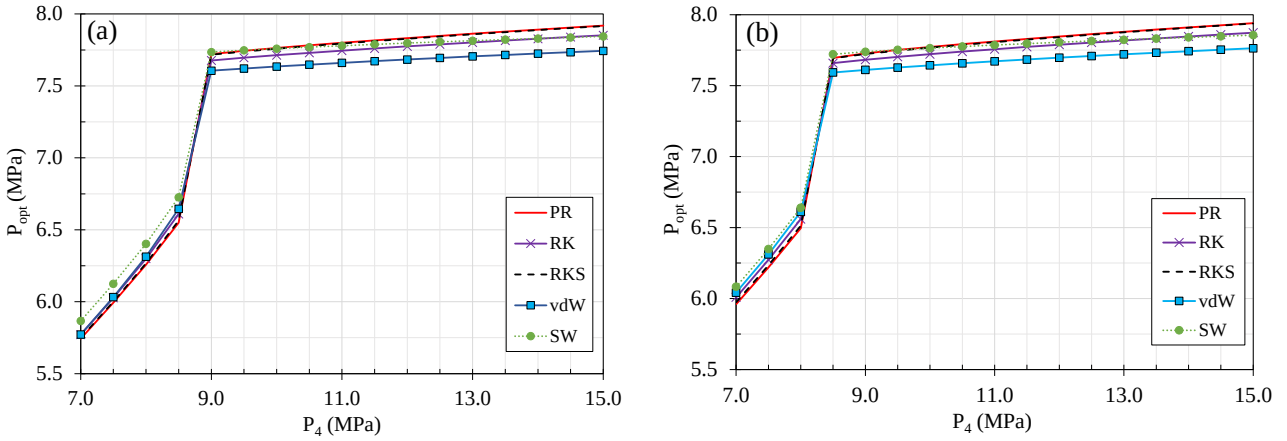

Figure 4 Optimum interstage pressures for CO_2 compression from P_1 = 2.6487 MPa, T_1= 264 K to different P_4 with T_3 = 306 K, (a) isentropic compression and (b) non-isentropic compression with $\eta_{isen,1} = 0.87$ and $\eta_{isen,2} = 0.82$

The optimum interstage pressure from the cubic and SW equations of state show the same shape for the isentropic and non-isentropic compressions, but they are different in values. Therefore, the discussions are done only for the isentropic compression. The optimum interstage pressure from the cubic and SW equations of state give a similar trend. For P_4 from 7.0 MPa to 9.0 MPa, the optimum interstage pressure dramatically increases with increasing P_4, especially with in the range of P_4 from 8.5 MPa to 9.0 MPa and from 8.0 MPa to 8.5 MPa for the isentropic and non-isentropic compressions, respectively. A 0.5 MPa increment in P_4 of theses ranges (8.5 MPa to 9.0 MPa and 8.0 MPa to 8.5 MPa) results in a nearly vertical ascent in the optimal interstage pressure changes. This rapid increase accidentally causes lines linking the optimal interstage pressures for these two points of P_4 to nearly overlap. However, it is important to inform that the optimal interstage pressure values within these P_4 ranges exhibit slight variations, similar to that occur at lower value of P_4. When the optimum interstage pressure is higher than the critical pressure, increasing P_4 causes a little increase of the optimal interstage pressure. The shape of the optimum interstage pressure as shown in Figures 4(a) and 4(b) has been found in Jeon and Kim's work [18] in which a multi-stage compression cycle of liquified CO_2 transport ship was studied.

For the comparison of the optimum interstage pressure obtained from the cubic equations of state and that from SW equation of stat, at P_4 lower than 8.5 MPa, SW equation of state gives the optimum interstage pressure higher than that from the cubic equations

of state. For higher P_4, the optimum interstage pressure from SW equation of state marginally changes when P_4 increases. However, the optimum interstage pressures from PR, RK and RKS equations of state increase with higher rates than that from SW equation of state. Therefore, the value of the optimum interstage pressure from SW equation of state varies between these values from PR, RK and RKS equations of state. PR and RKS equations of state give almost the same value of the optimum interstage pressure and they are averagely higher than that predicted by RK equation of state. The $AAPD$ for the case of PR, RK, and RKS equations of state are slightly different. These values are less than 0.9% and the highest value of $AAPD$ is found in the isentropic compression predicted by PR equation of state and its value is 0.88%. For vdW equation of state, it gives lowest optimal interstage pressure and finally approaches the value from SW equation of state. The $AAPD$ of the case of vdW equation of state is 1.46% for the isentropic compression and 1.27% for the non-isentropic compression.

To compare the results from the model developed in this study with that analyzed by Jeon and Kim [18], the optimum interstage pressures from the present model are plotted and compared with the results from [18], as illustrated in Figure 5. This figure shows that the optimum interstage pressures from using PR and RKS equations of state almost completely coincide with that from Jeon and Kim's analysis. The optimum interstage pressures from these two cubic equations of state compared to that from Jeon and Kim's work show $AAPD$ of 0.46% for RKS and 0.47% for PR equations of state. For the results using RK and vdW equations of state, they diverge from results of Jeon and Kim's analysis with $AAPD$ of 0.95% and 1.93%, respectively.

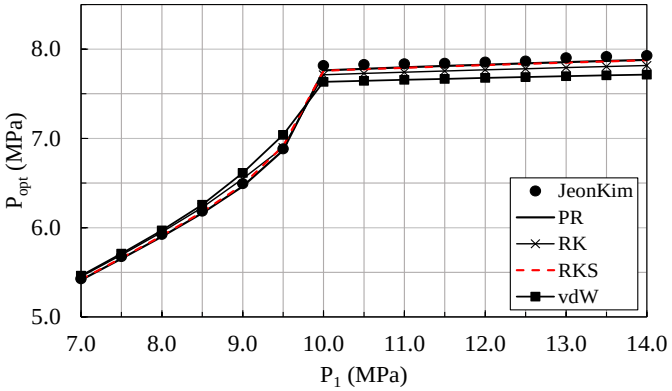

Figure 5 Comparison of optimum interstage pressure from present model and that from Ref. [18]

It is quite interesting that, in Figures 4(a), 4(b) and 5, after the optimum interstage pressure is higher than the critical pressure, when P_4 increases the optimum interstage pressure is almost unchanged. The reason is that the entropy constant lines around or on the left-hand side of the critical point are steeper than the others in the superheated region and the right-hand side of the critical point, as illustrated in P-h diagram shown in Figure 6. In the figure, it is the thermodynamic states plotted following the calculation of the optimum interstage pressure using PR equation of state for the case of $P_4 = 11.5$ MPa. The entropy constant line for the first-stage compression ($s = 1.90330$ kJ/kg·K) has lower slope than the entropy constant line for the second-stage compression ($s = 1.36792$ kJ/kg·K). It can be implied that when P_2 increases, the increase of the enthalpy change in the first-stage compression is more than the deduction of the enthalpy change in the second-stage compression due to different slope of entropy constant lines. Consequently, increase of the specific compression work in the first stage, $w_1 = (h_{2,s} - h_1)$, is more than reduction of the specific compression work in the second stage, $w_2 = (h_{4,s} - h_3)$. With similar reason, when P_4 increases, for example from 11.0 MPa to 11.5 MPa, the outlet pressure in the first-stage compression should slightly increases and the outlet pressure in the second-stage compression should be mainly increases to reach the desired P_4. Even though the pressure in the second-stage compression is mainly risen, the specific compression work in this stage slightly increases, because the entropy constant line is very steep and it causes a small increase of the enthalpy difference. For the non-isentropic compression, it can also be explained by this way, because the non-isentropic compression work is based on the isentropic compression work as $w_{act} = w_{isen}/\eta_{isen}$. However, if the isentropic efficiency of the second-stage compressor is much lower than that of the first-stage compressor, it possibly affects the changing trend of optimum interstage pressure.

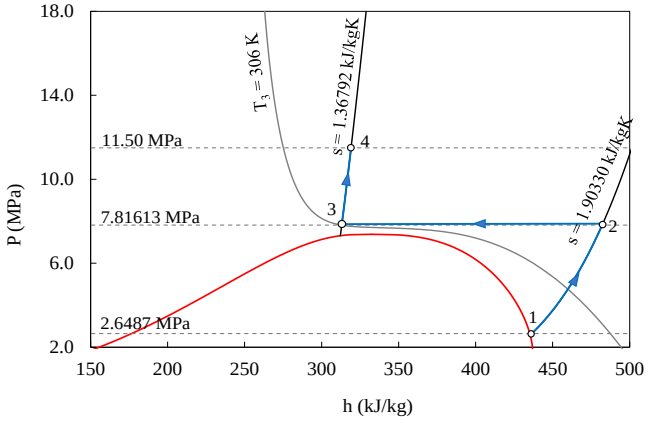

Figure 6 P-h diagram showing the thermodynamic states for the isentropic compression from P_1 = 2.6487 MPa, T_1 = 264 K to P_4 = 11.5 MPa with T_3 = 306 K

4. Conclusion

CO_2 compression is a key process in power generation and refrigeration systems using CO_2 as working fluid. Consequently, the optimum interstage pressures, minimizing compression work, is an interesting topic. The optimum interstage pressure model based on cubic equations of state for two-stage CO_2 compression is developed in this study. The results of the model are validated with the previous model using the multiparameter equation of state, called Span-Wagner (SW) equation of state. The developed model requires densities, temperatures and thermal expansivity to find the optimum interstage pressure. The main conclusions drawn from the study are summarized as follows:

- Cubic equations of state are computationally efficient because of their simplicity and they provide reasonably accurate properties even in supercritical region, especially RKS, PR, and RK equations of state.
- RKS, PR, and RK equations of state can predict the optimum interstage pressure close to that from the SW equation of state with the average absolute percentage difference less than 0.6% and 0.9% for subcritical and transcritical compressions, respectively.
- The ideal gas model cannot give the optimum interstage pressure with reasonable average absolute percentage difference, especially at high pressure.
- In transcritical compression, increase in outlet pressure of the second-stage compression causes a small increase in the optimum interstage pressure when the optimum interstage pressure is above the critical pressure. This is because the enthalpy difference in the first-stage compression is higher than that in the second-stage compression.

5. References

[1] Gür TM. Carbon dioxide emissions, capture, storage and utilization: review of materials, processes and technologies. Prog Energy Combust Sci. 2022;89:100965.

[2] Zhu C, Liu X, Xue S, He M. A comprehensive study on thermophysical properties of carbon dioxide through the cubic-plus-association and crossover cubic- plus-association equations of state. J Chem Eng Data. 2020;65(9):4268-84.

[3] Bai T, Shi R, Yu J. Thermodynamic performance evaluation of an ejector-enhanced transcritical CO_2 parallel compression refrigeration cycle. Int J Refrig. 2023;149:49-61.

[4] Li XL, Tang GH, Fan YH, Yang DL. A performance recovery coefficient for thermal-hydraulic evaluation of recuperator in supercritical carbon dioxide Brayton cycle. Energy Convers Manag. 2022;256:115393.

[5] Khatoon S, Kim MH. Preliminary design and assessment of concentrated solar power plant using supercritical carbon dioxide Brayton cycles. Energy Convers Manag. 2022;252:115066.

[6] Yin JM, Zheng QY, Peng ZR, Zhang XR. Review of supercritical CO_2 power cycles integrated with CSP. Int J Energy Res. 2020;44(3):1337-69.

[7] Niu H, Li W, Xiao H, Zhang X, Zhao K, Yang Z, et al. Numerical simulation of CO_2 two-stage compression refrigeration system with external intercooler. Int J Refrig. 2023;151:14-25.

[8] Çengel YA, Boles MA. Thermodynamics: an engineering approach. 8th ed. United States: McGraw-Hill; 2015.

[9] Klein S, Nellis G. Thermodynamics. United States: Cambridge University Press; 2012.

[10] Özgür AF. The performance analysis of a two-stage transcritical CO_2 cooling cycle with various gas cooler pressures. Int J Energy Res. 2008;32(14):1309-15.

[11] Agrawal N, Bhattacharyya S, Sarkar J. Optimization of two-stage transcritical carbon dioxide heat pump cycles. Int J Therm Sci. 2007;46(2):180-7.

[12] Vadasz P, Weiner D. The optimal intercooling of compressors by a finite number of interooolers. J Energy Resour Technol. 1922;114(3):255-60.

[13] Lugo-Méndez H, Lopez-Arenas T, Torres-Aldaco A, Torres-González EV, Sales-Cruz M, Lugo-Leyte R. Interstage pressures of a multistage compressor with intercooling. Entropy. 2021;23(3):351.

[14] López-Paniagua I, Rodríguez-Martín J, Sánchez-Orgaz S, Roncal-Casano JJ. Step by step derivation of the optimum multistage compression ratio and an application case. Entropy. 2020;22(6):678.

[15] Azizifar S, Banooni S. Modeling and optimization of industrial multistage compressed air system using actual variable effectiveness in hot regions. Adv Mech Eng. 2016;8(5):1-10.

[16] Jiang S, Wang S, Jin X, Yu Y. The role of optimum intermediate pressure in the design of two-stage vapor compression systems: a further investigation. Int J Refrig. 2016;70:57-70.

[17] Srinivasan K, Sheahen P, Sarathy CSP. Optimum thermodynamic conditions for upper pressure limits of transcritical carbon dioxide refrigeration cycle. Int J Refrig. 2010;33(7):1395-401.

[18] Jeon SH, Kim MS. Compressor selection methods for multi-stage re-liquefaction system of liquefied CO_2 transport ship for CCS. Appl Therm Eng. 2015;82:360-7.

[19] Cecchinato L, Chiarello M, Corradi M, Fornasieri E, Minetto S, Stringari P, et al. Thermodynamic analysis of different two-stage transcritical carbon dioxide cycles. Int J Refrig. 2009;32(5):1058-67.

[20] Span R, Wagner W. A new equation of state for carbon dioxide covering the fluid region from the triple-point temperature to 1100 K at pressures up to 800 MPa. J Phys Chem Ref Data. 1996;25(6):1509-96.

[21] Fang Y, De Lorenzo M, Lafon P, Poncet S, Bartosiewicz Y. An accurate and efficient look-up table equation of state for two-phase compressible flow simulations of carbon dioxide. Ind Eng Chem Res. 2018;57(22):7676-91.

[22] Reddy GJ, Basha H, Narayanan NSV. Transient natural convection heat transfer to CO_2 in the supercritical region. J Heat Transfer. 2018;140(9):092502.

[23] Jarungthammachote S. Optimal interstage pressures of multistage compression with intercooling processes. Therm Sci Eng Prog. 2022:29:101202.

[24] Mazzoccoli M, Bosio B, Arato E. Analysis and comparison of equations-of-state with p-rho-T experimental data for CO_2 and CO_2-mixture pipeline transport. Energy Procedia. 2012;23:274-83.

[25] Wang Z, Sun B, Yan L. Improved density correlation for supercritical CO_2. Chem Eng Technol. 2015;38(1):75-84.

[26] Zarei F, Baghban A. Estimating density of supercritical carbon dioxide and methane using modified thermodynamic models. Pet Sci Technol. 2018;36(6):437-42.

[27] Zhao Q, Mecheri M, Neveux T, Privat R, Jaubert JN. Selection of a proper equation of state for the modeling of a supercritical CO_2 Brayton cycle: consequences on the process design. Ind Eng Chem Res. 2017;56(23):6841-53.
[28] Leal DS, Embiruçu M, Costa GMN, Pontes KV. Prediction of thermodynamic properties of CO_2 by cubic and multiparameter equation of state for fluid dynamics applications. J Chem Eng Data. 2019;64(4):1746-59.
[29] Ramos Figueroa AL, Carreño-Chávez RA, Estévez LA. Thermal expansivity of near- and supercritical fluids: equation-of-state models and calculations for carbon dioxide and C1 to C4 normal alkanes. J Chem Eng Data. 2019;64(5):2126-33.
[30] McBride BJ, Zehe MJ, Gordon S. NASA Glenn coefficients for calculating thermodynamic properties of individual species. NASA/TP—2002-211556. United States: National Aeronautics and Space Administration; 2002.
[31] Fenghour A, Wakeham WA, Watson JTR. Amount-of-substance density of CO_2 at temperatures from 329 K to 698 K and pressures up to 34 MPa. J Chem Thermodyn. 1995;27(2):219-23.
[32] Duschek W, Kleinrahm R, Wagner W. Measurement and correlation of the (pressure, density, temperature) relation of carbon dioxide I. The homogeneous gas and liquid regions in the temperature range from 217 K to 340 K at pressures up to 9 MPa. J Chem Thermodyn. 1990;22(9):827-40.
[33] Klimeck J, Kleinrahm R, Wagner W. Measurements of the (p, ρ, T) relation of methane and carbon dioxide in the temperature range 240 K to 520 K at pressures up to 30 MPa using a new accurate single-sinker densimeter. The Journal of Chemical Thermodynamics. 2001;33(3):251-67.

Appendix A. Derivation of Eq. (5)

Based on the total specific work defined in Eq. (4) and the assumption that the isentropic efficiencies are constants, the derivative of the total specific work with respect to P_2 can be expressed as:

$$\frac{\partial w_{tot}}{\partial P_2}=\frac{1}{\eta_{isen2}}\frac{\partial}{\partial P_2}\left(h_{4,s}-h_3\right)+\frac{1}{\eta_{isen1}}\frac{\partial}{\partial P_2}\left(h_{2,s}-h_1\right) \tag{App. 1}$$

The derivative of h_1 with respect to P_2 , $(\partial h_1/\partial P_2)$, is zero because the compressor inlet state or state 1 is independent of the pressure P_2. The temperature T_3 and the desired discharge pressure, P_4, are known parameters. The derivative of $h_{4,s}$ with respect to P_2 , $\left(\partial h_{4,s}/\partial P_2\right)$, can be transformed as $\left(\partial h_{4,s}/\partial s_4\right)_{P=P_4} \times \left(\partial s_3/\partial P_2\right)_{T=T_3}$. As it requires a lot of page space to describe, a detailed explanation of this transformation can be found in Ref. [23]. Therefore, Eq. (App. 1) can be rewritten as the following equation.

$$\frac{\partial w_{tot}}{\partial P_2}=\frac{1}{\eta_{isen2}}\left[\left(\frac{\partial h_{4,s}}{\partial s_4}\right)_{P=P_4}\left(\frac{\partial s_3}{\partial P_2}\right)_{T=T_3}-\left(\frac{\partial h_3}{\partial P_2}\right)_{T=T_3}\right]+\frac{1}{\eta_{isen1}}\left(\frac{\partial h_{2,s}}{\partial P_2}\right)_{s=s_1} \tag{App. 2}$$

From the Maxwell relationship, it gives that $\left(\partial h_{4,s}/\partial s_4\right)_{P=P_4}=T_4$, $\left(\partial h_{2,s}/\partial P_2\right)_{s=s_2}=1/\rho_2$ and $(\partial h_3/\partial P_2)_{T=T_3}=T_3(\partial s_3/\partial P_2)_{T=T_3}+1/\rho_3$. No pressure drop in the intercooling is assumed. It results in that $P_2=P_3$. Substituting these relations into Eq. (App. 2) and set the result to be zero, it yields:

$$\frac{1}{\eta_{isen2}}\left[T_4\left(\frac{\partial s_3}{\partial P_3}\right)_{T=T_3}-T_3\left(\frac{\partial s_3}{\partial P_3}\right)_{T=T_3}-\frac{1}{\rho_3}\right]+\frac{1}{\eta_{isen1}}\frac{1}{\rho_2}=0 \tag{App. 3}$$

Arranging Eq. (App. 3) gives Eq. (App. 4) which is similar to Eq. (5).

$$\frac{T_4-T_3}{\eta_{isen2}}-\frac{\left[1/(\rho_3\eta_{isen2})-1/(\rho_2\eta_{isen1})\right]}{\left(\partial s_3/\partial P_3\right)_{T=T_3}}=0 \tag{App. 4}$$